The Plant Cell, Vol. 18, 2999–3014, November 2006, www.plantcell.org © 2006 American Society of Plant Biologists

The Rice *Tapetum Degeneration Retardation* Gene Is Required for Tapetum Degradation and Anther Development [W]

Na Li,[a,b,1] Da-Sheng Zhang,[a,1] Hai-Sheng Liu,[a] Chang-Song Yin,[a] Xiao-xing Li,[a] Wan-qi Liang,[a] Zheng Yuan,[a] Ben Xu,[c] Huang-Wei Chu,[a] Jia Wang,[a] Tie-Qiao Wen,[b] Hai Huang,[c] Da Luo,[c] Hong Ma,[a,c,d] and Da-Bing Zhang[a,c,2]

[a] Shanghai Jiao Tong University–Shanghai Institutes for Biological Sciences–Pennsylvania State University Joint Center for Life Sciences, School of Life Science and Biotechnology, Key Laboratory of Microbial Metabolism, Ministry of Education, Shanghai Jiao Tong University, Shanghai 200240, China

[b] College of Life Science, Shanghai University, Shanghai 200436, China

[c] Institute of Plant Physiology and Ecology, Shanghai Institutes for Biological Sciences, Chinese Academy of Sciences, Shanghai 200032, China

[d] Department of Biology, Huck Institutes of the Life Sciences, Pennsylvania State University, University Park, Pennsylvania 16082

In flowering plants, tapetum degeneration is proposed to be triggered by a programmed cell death (PCD) process during late stages of pollen development; the PCD is thought to provide cellular contents supporting pollen wall formation and to allow the subsequent pollen release. However, the molecular basis regulating tapetum PCD in plants remains poorly understood. We report the isolation and characterization of a rice (*Oryza sativa*) male sterile mutant *tapetum degeneration retardation* (*tdr*), which exhibits degeneration retardation of the tapetum and middle layer as well as collapse of microspores. The *TDR* gene is preferentially expressed in the tapetum and encodes a putative basic helix-loop-helix protein, which is likely localized to the nucleus. More importantly, two genes, Os *CP1* and Os *c6*, encoding a Cys protease and a protease inhibitor, respectively, were shown to be the likely direct targets of TDR through chromatin immunoprecipitation analyses and the electrophoretic mobility shift assay. These results indicate that *TDR* is a key component of the molecular network regulating rice tapetum development and degeneration.

INTRODUCTION

The life cycle of flowering plants alternates between diploid sporophyte and haploid gametophyte generations. Male gametophytes develop in the anther compartment of the stamen within the flower, the sporophytic reproductive structure, and require cooperative functional interactions between gametophytic and sporophytic tissues (Scott et al., 1991; Goldberg et al., 1993; McCormick, 1993; Raghavan, 1997; Ma, 2005). The anther has four lobes that are similar in structure and are attached to a central core with connective and vascular tissues. When anther morphogenesis is complete, the meiotic cells (also called microsporocytes) at the center of each anther lobe are surrounded by four somatic layers, which are, from the surface to interior, the epidermis, endothecium, middle layer, and tapetum (Goldberg et al., 1993). As the innermost of the four sporophytic layers of the anther wall, the tapetum directly contacts with the developing gametophytes and plays a crucial role in the development from microspore to pollen grains (Pacini et al., 1985; Shivanna et al., 1997). As a secretory cell layer, the tapetum provides enzymes for the release of microspores from tetrads and nutrients for pollen development (Goldberg et al., 1993).

It is known that the tapetum undergoes cellular degradation during late stages of pollen development. This degradation process is considered to be a programmed cell death (PCD) event (Papini et al., 1999; Wu and Cheung, 2000). At the structural level, the tapetum PCD is characterized by sequential elimination of the cellular structures. For example, in both *Lobivia rauschii* and *Tillandsia albida*, the cytological features of tapetum PCD include cytoplasmic shrinkage, oligonucleosomal cleavage of DNA, vacuole rupture, and swelling of the endoplasmic reticulum (Papini et al., 1999). Tapetal cell differentiation and subsequent disintegration coincides very well with the anther postmeiotic developmental program, and premature or delayed degradation of tapetum is associated with male sterility.

Molecular genetic studies have identified a few genes that control the formation of tapetum (Ma, 2005), including the *Arabidopsis thaliana EXCESS MICROSPOROCYTES1* (*EMS1*)/*EXTRA SPOROGENOUS CELLS* (*EXS*) gene encoding a leucine-rich repeat (LRR) receptor-like protein kinase (Canales et al., 2002; Zhao et al., 2002) and the *TAPETAL DETERMINANT1* gene encoding a putative small secreted protein (Yang et al., 2003, 2005; Ma, 2005). Recently, two highly similar *Arabidopsis* LRR receptor-like protein kinases, SOMATIC EMBRYOGENESIS RECEPTOR KINASE1 (SERK1) and SERK2, were found to be required in tapetum formation in a way similar to that of EMS1/EXS (Albrecht et al., 2005; Colcombet et al., 2005). In rice (*Oryza sativa*), the *MULTIPLE SPOROCYTE1* gene encodes an LRR

[1] These authors contributed equally to this work.

[2] To whom correspondence should be addressed. E-mail zhangdb@sjtu.edu.cn; fax 86-21-34204869.

The author responsible for distribution of materials integral to the findings presented in this article in accordance with the policy described in the Instructions for Authors (www.plantcell.org) is: Da-Bing Zhang (zhangdb@sjtu.edu.cn).

[W] Online version contains Web-only data.

www.plantcell.org/cgi/doi/10.1105/tpc.106.044107

receptor-like protein kinase that is highly similar to EMS1 and has a function resembling that of EMS1/EXS (Nonomura et al., 2003). More recently, the rice *Undeveloped Tapetum1* (*Udt1*) gene was shown to be important for tapetum differentiation and the formation of microspores (Jung et al., 2005).

Other genes have been shown to affect postmeiotic tapetum development and/or function and microspore development. For instance, the *Arabidopsis ABORTED MICROSPORE* (*AMS*) gene encoding a basic helix-loop-helix (bHLH)–containing protein plays a crucial role in tapetum and microspore development (Sorensen et al., 2003). In addition, the *Arabidopsis MALE STERILITY1* gene encodes a protein with a PHD finger and is important for proper tapetum function and normal microspore development (Wilson et al., 2001). Moreover, At *MYB103* is required for the development of tapetum, pollen, and trichome (Higginson et al., 2003). In *Penutia hybrida*, the tapetum-specific zinc finger gene *TAZ1* is important for postmeiotic tapetum development (Kapoor et al., 2002).

On the other hand, little is known about the genetic basis regulating PCD of tapetum during late pollen development. In this report, we describe the isolation and characterization of a rice male sterile *tapetum degeneration retardation* (*tdr*) mutant with a mutation in a putative bHLH transcription factor gene. In the *tdr* anther, the tapetum PCD was retarded and the middle layer cells persisted, accompanied by aborted pollen development and complete male sterility. Furthermore, *TDR* is expressed highly preferentially in the tapetal cells, suggesting that *TDR* acts within the tapetum to promote its normal development and postmeiotic degradation. *TDR* encodes a putative transcription factor with a bHLH domain. Moreover, using chromatin immunoprecipitation (ChIP) and electrophoretic mobility shift assay (EMSA), we show that two genes, Os *CP1* and Os *c6*, encoding a Cys protease and a protease inhibitor, respectively, are likely direct targets of TDR. These results provide important insights into the crucial role of TDR in a transcriptional regulatory network for tapetum development and degradation.

RESULTS

Isolation and Phenotypic Analyses of the *tdr* Mutant

To identify rice genes that are important for the regulation of anther development, we generated a rice mutant library of the *japonica* subspecies using γ-ray radiation and found the *tdr* mutant by its complete male sterility. Genetic analysis indicated that a single recessive nuclear locus controlled the mutant phenotype (Liu et al., 2005). The *tdr* plant was normal in vegetative and floral development but failed to produce any viable pollen (Figures 1A to 1D). Compared with wild-type anthers, the mutant anthers were small and white, without mature pollen grains (cf. Figures 1E to 1H).

To determine the anther morphological defects in the *tdr* mutant, anther transverse sections were further examined.

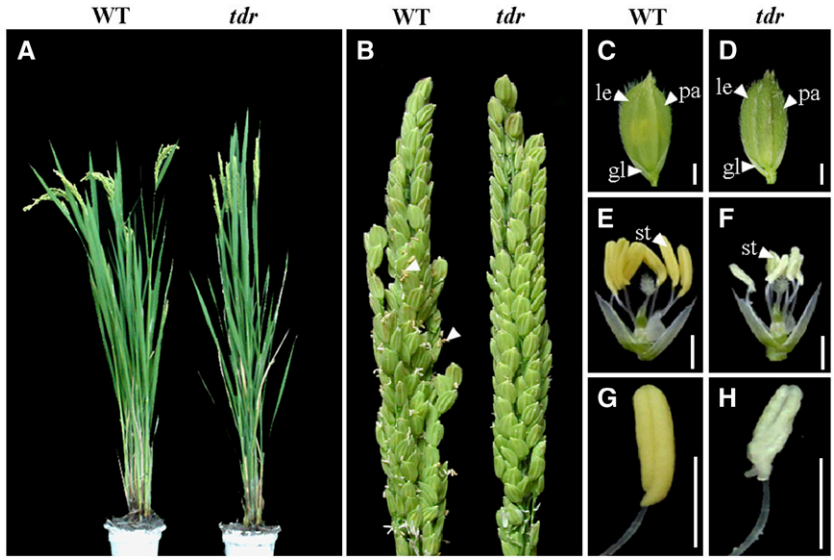

Figure 1. Comparison of the Wild Type and the *tdr* Mutant.

(A) Comparison of a wild-type plant (left) and a *tdr* mutant plant (right) after bolting.
(B) Comparison of a wild-type panicle (left) and a *tdr* mutant panicle at the heading stage.
(C) A wild-type spikelet.
(D) A mutant spikelet.
(E) A wild-type spikelet after removing the lemma and palea.
(F) A mutant spikelet after removing the lemma and palea.
(G) A wild-type yellow anther.
(H) A mutant white and smaller anther.
le, lemma; pa, palea; gl, glume; st, stamen. Bars = 2 mm.

Based on the cellular events visible under the light microscope and previous classification of anther development (Feng et al., 2001), we divided rice anther development into eight stages. During the early premeiosis stage, the archesporial cells divided to form primary parietal cells and primary sporogenous cells. The primary sporogenous cells then divided to generate the sporogenous cells, and the primary parietal cells divided to form a layer of endothecial cells and a layer of secondary parietal cells. There was no detectable difference between the wild type and the *tdr* anthers at this stage (Figures 2A and 2B). Up to the microspore mother cell (MMC) stage, there was still no obvious difference in anther cellular morphology between the wild type and *tdr*. Normal epidermis, endothecium, middle layer, tapetum, and microsporocytes were found in both wild-type and the *tdr* anthers (Figures 2C and 2D).

Subsequently, the *tdr* mutant anther had detectable morphological abnormalities. During the meiosis stage, wild-type MMCs underwent meiosis to form tetrads of four haploid microspores. The tapetal cells then differentiated and their cytoplasm became deeply stained, while the middle layer cells became very thin and degenerated (Figure 2E). In the *tdr* anther, microsporocytes seemed normal and could undergo meiosis to form tetrads, as observed using 4′,6-diamidino-2-phenylindole staining (see Supplemental Figure 1 online). However, the cytoplasm of tapetum and middle layer cells in the *tdr* mutant were not deeply stained (Figure 2F). At the tetrad stage, wild-type meiocytes had formed tetrads, the tapetal cytoplasm continued to agglomerate, and the middle layer assumed a band-like shape (Figure 2G). In the *tdr* anther, although the tetrads had formed, the tapetum seemed to be vacuolated and the middle layer remained relatively

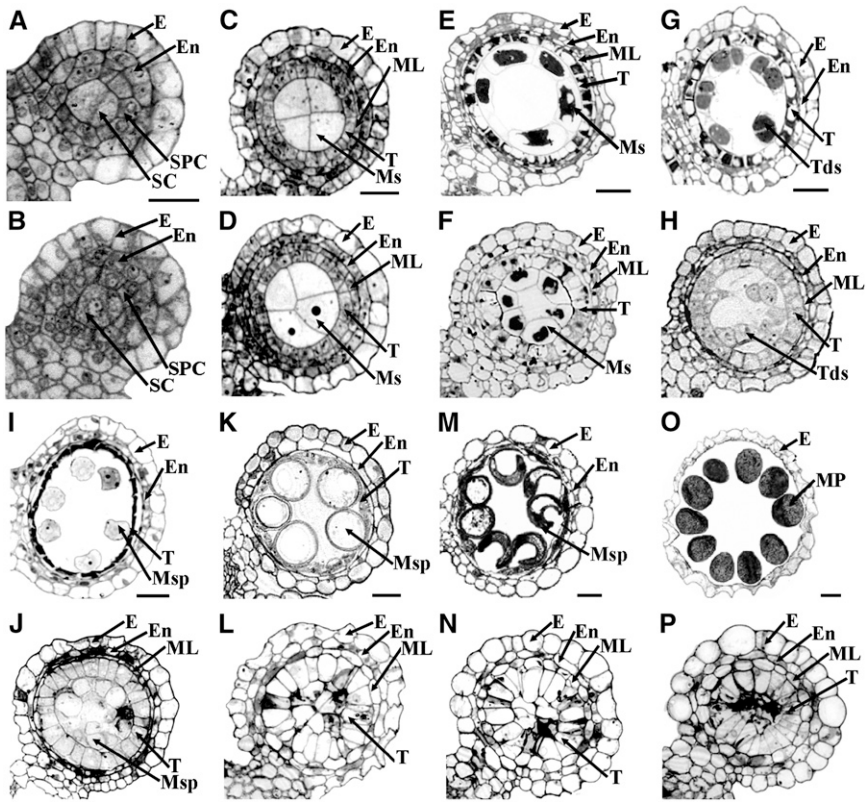

Figure 2. Transverse Section Comparison of the Anther Development of the Wild Type and the *tdr* Mutant.

Eight stages of anther development in the wild type and the corresponding stages of development in the *tdr* mutant were compared. The images are of cross sections through single locules. Wild-type sections are shown in **(A)**, **(C)**, **(E)**, **(G)**, **(I)**, **(K)**, **(M)**, and **(O)**, and other panels show *tdr* sections. E, epidermis; En, endothecium; ML, middle layer; T, tapetum; Ms, microsporocyte; Tds, tetrads; Msp, microspore; MP, mature pollen; SPC, secondary parietal cell; SC, sporogenous cell. Bars = 15μm.

(A) and **(B)** The early premeiosis stage.
(C) and **(D)** The MMC stage.
(E) and **(F)** The late meiosis stage.
(G) and **(H)** The tetrad stage.
(I) and **(J)** The young microspore stage.
(K) and **(L)** The vacuolated pollen stage.
(M) and **(N)** The pollen mitosis stage.
(O) and **(P)** The mature pollen stage.

thick (Figure 2H). Subsequently, at the young microspore stage in wild-type anthers, microspores were released from tetrads, tapetal cells had deeply stained cytoplasm but no longer had large vacuoles, and the middle layer was hardly visible (Figure 2I). By contrast, the *tdr* tapetal cells continued to expand and remained vacuolated, and the middle layers were still clearly visible (Figure 2J). From the vacuolated pollen stage to the pollen mitosis stage, wild-type pollen exine deposition was completed, and the uninucleate pollen developed to trinucleate pollen through two mitotic divisions, while the tapetal cells differentiated and degenerated (Figures 2K and 2M). However, the *tdr* mutant microspores collapsed following release from tetrads. The middle layer and tapetum became more vacuolated and expanded (Figures 2L and 2N). At the mature pollen stage, wild-type pollen grains were full of starch, lipids, and other nutrients, and the tapetum was fully degenerated (Figure 2O). However, the *tdr* microspores were completely degenerated with only densely staining remnants at the center of the anther locule, whereas tapetum cells became abnormally large and extremely vacuolated and occupied the majority of locule. The middle layer did not degenerate (Figure 2P).

To gain a more detailed understanding of the abnormalities of the *tdr* tapetal cells, we used transmission electron microscopy (TEM) to study the mutant anther. At the early meiosis stage, there were no distinct differences between wild-type and the *tdr* mutant anthers (Figures 3A and 3B). At the tetrad stage, the tetrad was formed in wild-type anthers through meiosis, and the cytoplasm of tapetal cell was condensed and deeply stained (Figures 3C and 3E). Also, tetrads also could be observed in the *tdr* mutant anther. However, the cytoplasm of the *tdr* tapetal cell was not as darkly stained as that of the wild-type tapetum (Figures 3D and 3F). At the young microspore stage, wild-type tapetal cells became collapsed in conjunction with the dissolution of cell walls, as is typical for the secretory tapetum in angiosperms and crucial for supplying nutrition to the developing microspores (Figure 3G). By contrast, the *tdr* tapetal cells became enlarged with large vacuoles and did not degenerate (Figure 3H). Consistent with previous results (Owen and Makaroff, 1995), the wild-type tapetal cells at this stage had significant dilation of endoplasmic reticulum cisternae consisting of >12 layers. Mitochondria could be recognized as having an electron-dense matrix and enlarged cristae, and the nucleus of the tapetal cell was lobed. All of these signified cellular degeneration in the wild-type tapetal cell during the tetrad stage (Figure 3I). However, in the *tdr* mutant, the tapetal cytoplasm was full of high electron density matrix, and the nucleus showed no shrinkage. The endoplasmic reticulum dilation in *tdr* tapetal cells was greatly reduced, unusual patterns of endoplasmic reticulum could be observed occasionally, and the mutant mitochondria lost its normal features with reduced cristae (Figure 3J). Therefore, the wild-type tapetal cells at the young microspore stage show distinct characteristics of cellular degeneration; however, the lack of ultrastructural characteristics of degeneration in the *tdr* tapetal cells indicates their failure to degrade. Meanwhile, the *tdr* tapetum cytological abnormalities were accompanied by structural defects in microspores. At the young microspore stage, the spherical wild-type microspores contained mitochondria, plastids, and vacuoles distributed around the endoplasmic reticulum (Figure 3K). The exine of wild-type pollen was established with distinct tectum, bacula, and nexine layers (Figure 3M). However, the *tdr* microspore was abnormal in shape, with irregularly distributed vacuoles and reduced endoplasmic reticulum (Figure 3L). Particularly, there was no detectable exine (Figure 3N). At the vacuolated pollen stage, further degenerated tapetum and vacuolated microspores were observed in the wild-type anthers (Figure 3O). However, at this stage, the extremely expanded tapetal cell occupied the majority of the locule, and microspores entirely collapsed (Figure 3P). These observations suggest that the *tdr* mutation resulted in the defects in tapetum degeneration, further affecting microspore development, particularly exine formation.

Loss of *TDR* Function Causes Aborted Tapetal PCD

The phenotypic analysis described above suggests that the *tdr* mutation affected the differentiation and degradation of tapetal cells. In plants, the degeneration of tapetum is considered to be the result of PCD, which is characterized by the cleavage of nuclear DNA. To test whether the *tdr* mutant anthers are defective in PCD, we performed the TUNEL (for terminal deoxynucleotidyl transferase–mediated dUTP nick-end labeling) assay in wild-type and the *tdr* anthers. A range of developmental stages was analyzed, including meiosis stage, tetrad stage, microspore stage, and vacuolated pollen stage from the wild type and the corresponding stages selected from the *tdr* mutant. During the meiosis stage, both wild-type and the *tdr* tapetal cells showed TUNEL-negative nuclei (Figures 4A and 4B), indicating lack of DNA fragmentation at this stage. At the tetrad stage, the TUNEL-positive nuclei were detected in wild-type tapetal cells, suggesting that PCD occurred in the tapetum (Figure 4C). However, little fragmented DNA signal was observed in the *tdr* mutant anthers at this stage (Figure 4D). Wild-type anthers at the young microspore stage showed more strong TUNEL-positive signals in tapetal cells. Simultaneously, the TUNEL signals were also observed in the outer cell layers of the anther (endothecium and middle layer) and vascular bundle cells (Figure 4E). However, TUNEL fluorescence signal was still not detected in the *tdr* tapetum at the young microspore stage (Figure 4F). At the vacuolated pollen stage, TUNEL-positive nuclei were present in degenerating tapetal cells and stomium cells in wild-type anthers (Figure 4G), and a weak signal could be observed in the expanded tapetal cells and collapsed microspores in the *tdr* mutant (Figure 4H). These observations demonstrate that the PCD of tapetum commences at the tetrad stage in wild-type anther, and the retardation of PCD in tapetum possibly results in the failure of tapetum degeneration in the *tdr* mutant.

To quantify the results from the TUNEL assay, we compared DNA damage levels between the wild-type and the *tdr* mutant anthers using the comet assay (Wang and Liu, 2006). The *tdr* mutant anthers at the MMC stage exhibited similar levels of DNA damage to those of the wild type. From the tetrad stage to vacuolated pollen stage, wild-type anthers exhibited significant increases in DNA damage. However, the *tdr* mutant anthers exhibited lower than normal levels of DNA damage from the tetrad stage to the vacuolated pollen stage (Figure 5). The result of the comet assay also confirmed the retardation of PCD in the *tdr* anthers.

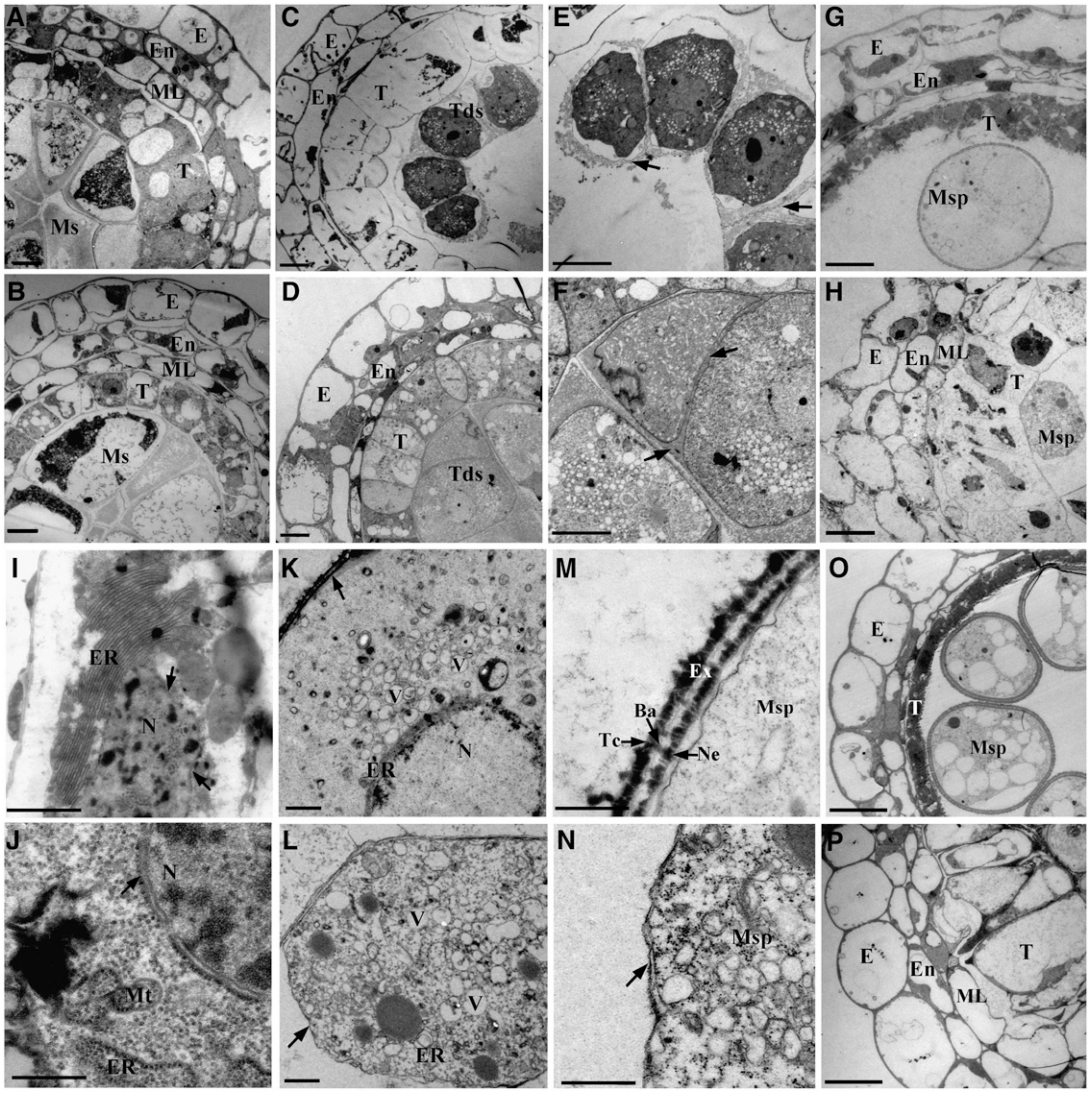

Figure 3. Transmission Electron Micrographs of the Anthers from the Wild Type and the *tdr* Mutant.

(A) The early meiosis stage wild-type anther showing microsporocyte.
(B) The *tdr* mutant anther at early meiosis stage showing microsporocyte.
(C) The tetrad stage wild-type anther showing tetrad.
(D) The *tdr* mutant anther at the tetrad stage showing tetrad.
(E) A higher magnification of tetrad in **(C)** showing callose (arrows).
(F) A higher magnification of tetrad in **(D)** showing callose (arrows).
(G) The young microspore stage wild-type anther showing highly condensed tapetal cytoplasm and spherical microspores.
(H) The young microspore stage of the *tdr* mutant anther showing the hypertrophy of tapetal cells and abnormal microspores.
(I) Wild-type tapetal cytoplasm showing dilation of the endoplasmic reticulum and lobed nucleus (arrows).
(J) The *tdr* mutant tapetal cytoplasm showing unusual pattern of the endoplasmic reticulum, abnormal mitochondria, and intact nucleus membrane (arrow).
(K) Wild-type microspore showing the endoplasmic reticulum and developing vacuoles being distributed all around the ER. Arrow shows the exine.
(L) The *tdr* mutant microspore with abnormal shape and more irregularly distributed vacuoles. Arrow indicates the exine.
(M) Higher-magnification view of the exine in **(K)** showing tectum, bacula, and nexine (arrows).
(N) The *tdr* mutant microspore with coarse primexine (arrow).
(O) The vacuolated pollen stage wild-type anther showing degenerated tapetum and vacuolated microspores.
(P) The *tdr* mutant anther at the vacuolated pollen stage showing overly expanded tapetum.
E, epidermis; En, endothecium; ML, middle layer; T, tapetum; Ms, microsporocyte; Tds, tetrads; Msp, microspore; Mt, mitochondria; ER, endoplasmic reticulum; V, vacuole; N, nucleus; Ex, exine; Tc, tectum; Ba, bacula; Ne, nexine. Bars = 5 μm in **(A)** to **(H)**, **(O)**, and **(P)**, 1 μm in **(K)** and **(L)**, and 0.5 μm in **(I)**, **(J)**, **(M)**, and **(N)**.

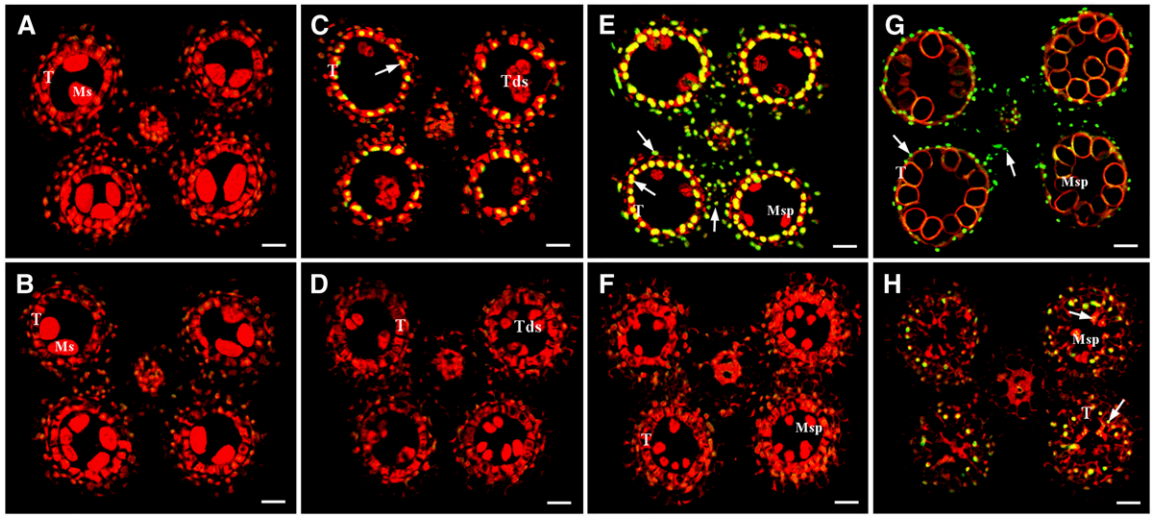

Figure 4. DNA Fragmentation in Wild-Type and *tdr* Mutant Anthers.

The anthers of the four developmental stages in the wild type and the *tdr* mutant were compared for nuclear DNA fragmentation using the TUNEL assay. Nuclei have been stained with propidium iodide indicated by red fluorescence, while yellow to green fluorescence is TUNEL-positive nuclei staining. T, tapetum; Ms, microsporocyte; Tds, tetrads; Msp, microspore. Bars = 50 μm.

(A) The wild type at meiosis stage.

(B) The *tdr* mutant at meiosis stage.

(C) Wild-type anther at tetrad stage showing TUNEL-positive signal in tapetal cells (arrow).

(D) The *tdr* mutant at tetrad stage.

(E) The wild type at young micropsore stage. TUNEL-positive signal is detected in the tapetum, outer cell layers, and vascular bundle cells (arrows).

(F) The *tdr* mutant at young microspore stage.

(G) Wild-type anther at the vacuolated pollen stage showing TUNEL-positive signal in the tapetal cells and stomium area (arrows).

(H) The *tdr* mutant at vacuolated pollen stage. TUNEL-positive signal is detected in expanded tapetal cells and collapsed microspores (arrows).

Isolation of the *TDR* Gene

The *TDR* locus was previously mapped to the short arm of rice chromosome 2 between the two InDel molecular markers LHS10 and LHS6 with a physical distance of 133 kb (Liu et al., 2005). To further map the *TDR* gene, we generated a large F2 mapping population, and 2450 segregants showing the *tdr* mutant phenotype were analyzed. The *TDR* gene was located between two newly developed InDel markers LHS12 and LHS3 defining a region of 52 kb (Figure 6A). Through repeated sequencing, we confirmed a single nucleotide deletion in the seventh exon of an annotated bHLH gene (Os02g02820), which caused a frame shift and premature translational termination (Figure 6B). The Os02g02820 gene was confirmed to be *TDR* by a functional complementation experiment. A binary plasmid carrying a 6.4-kb wild-type *Bam*HI-*Sal*I genomic fragment from the BAC clone AP005851 was able to rescue the sterile phenotype of the *tdr* homozygous plants (see Supplemental Figure 2 online).

The *TDR* open reading frame encodes a putative bHLH protein of 552 amino acids with a bHLH domain between the 280th and 341st amino acids (Figure 6C). The presence of a potential nuclear localization signal (RKRRKK, amino acids 290 to 296) in the TDR protein suggests that TDR protein is possibly targeted to the nucleus (Figure 6C). To determine the subcellular localization of TDR, we constructed a translation fusion between the cDNA for the green fluorescent protein (GFP) and the full-length *TDR* coding region. The *TDR-GFP* fusion construct and the *GFP* alone control, both driven by the *35S* promoter, were introduced into onion epidermal cells by particle bombardment. As expected, the free GFP was found in the nucleoplasm and in the cytoplasm (Figure 6D). By contrast, the TDR-GFP fusion protein was observed exclusively in the nucleus (Figure 6E). Nuclear-localizing AS2 was used as a positive control, and AS2-GFP fusion protein was observed specifically in the nucleus (Figure 6F). These results suggest that TDR is localized to the nucleus.

Sequence Analysis of TDR and Related Proteins

To gain additional insights into the phylogenetic relationship between TDR and its close homologs, we searched public databases using BLAST with the TDR sequence as a query. The full-length amino acid sequences of TDR and its 12 closest homologs were used for phylogenetic analysis. Our result revealed that *TDR* and *Arabidopsis AMS* (Sorensen et al., 2003) were supported as an orthologous pair (Figure 7A). Furthermore, sequence comparison indicated that TDR shares 32% overall identity with *Arabidopsis* AMS (Figure 7B). In *Arabidopsis*, the *ams* mutation results in abnormal tapetum expansion and persistence of middle layer, which is similar to the phenotype of the *tdr* mutant. However, PCD was not analyzed in the *ams* mutant.

Additionally, the rice *Udt1* gene also encodes a bHLH protein, which plays a major role in maintaining rice tapetum development

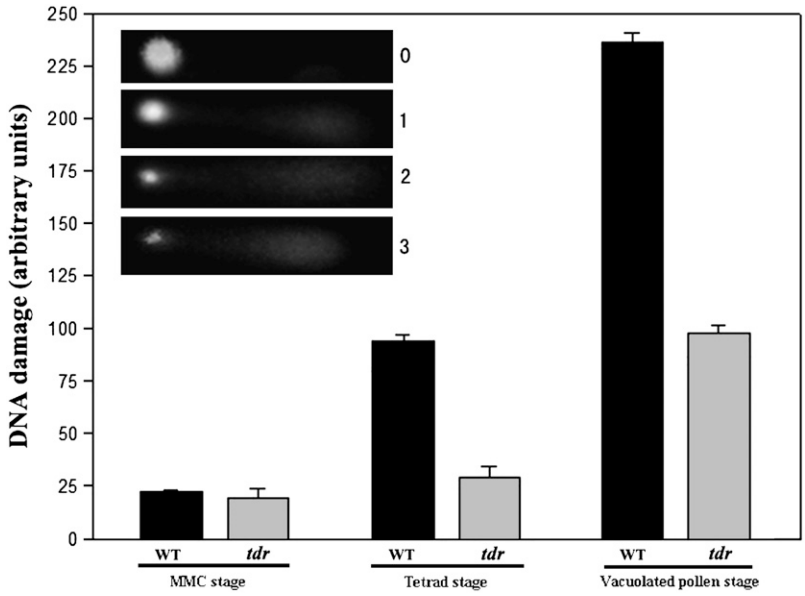

Figure 5. Analyses of DNA Damage in the Wild Type and the *tdr* Mutant Anther Tissues.

Comet assay used to assess the relative amount of DNA damage in the wild type and the *tdr* mutant anther at different stages. The *tdr* mutant anthers at the MMC stage exhibited similar levels of DNA damage to those of the wild type. The DNA damage level in the wild type was increased from the tetrad stage and reached the maximum at the vacuolated pollen stage. The *tdr* mutant exhibited an increased level of DNA damage just from the vacuolated pollen stage. The extent of DNA damage in each nucleus is indicated by the units 0, 1, 2, or 3. An increased unit correlated with a higher DNA percentage in tail, as illustrated in the inset. This assignation was described by Wang and Liu (2006). The DNA damage units were obtained by summing the units from 100 nuclei on each slide. Bars indicate SD.

at the early meiosis stage (Jung et al., 2005). Comparative analysis revealed that the full-length amino acid sequences between the TDR and Udt1 have only 12% identity (Figure 7B). In the *udt1* mutant, the transcript of *TDR* is reduced (Jung et al., 2005), while the *tdr* mutation has no obvious effect on the expression of *Udt1* (see Supplemental Figure 4 online). So, the *Udt1* gene probably acts upstream of *TDR*.

TDR Is Preferentially Expressed in the Tapetum

The *tdr* mutation affected the tapetum postmeiotic degeneration and the morphology of other anther wall cells and microspores but had little effect on rice vegetative growth and other flower organ development. To test whether *TDR* acts within the anther or from a distant tissue, we analyzed the *TDR* expression pattern.

We first detected *TDR* expression by RT-PCR with total RNA extracted from vegetative and reproductive organs (Figure 8A). There was no detectable expression of *TDR* in vegetative and floral organs other than the anther. By contrast, *TDR* expression was clearly detected at relatively early stages of anther development, starting at the meiosis stage and reaching the maximum level at the young microspore stage. When the young microspores developed into the vacuolated pollen stage, the transcript level of *TDR* was greatly reduced. At the heading stage, the *TDR* transcripts were hardly detectable.

To more precisely determine the spatial and temporal patterns of *TDR* expression, we performed RNA in situ hybridization with wild-type floral sections (Figures 8B to 8G). At the early premeiosis stage, the *TDR* transcript was hardly detectable (Figure 8B). The *TDR* transcripts were initially detected in the tapetal, middle layer, and endothecium of the meiosis stage anthers (Figure 8D). At the tetrad stage, the *TDR* gene was more strongly expressed in the tapetum (Figure 8F). Only background levels of signal were detected with the sense probe (Figures 8C, 8E, and 8G). Endo et al. (2004) showed that *TDR* (Os02g02820) was mainly expressed in the tapetum at the young microspore stage through in situ hybridization probed with another DNA fragment of *TDR*. Therefore, *TDR* expression is associated with the differentiation of tapetal cells during rice anther development.

TDR Interacts with Os *CP1* and Os *c6*

TDR is a putative bHLH transcription factor expected to regulate gene expression by binding to an E-box (CANNTG) (Bouchard et al., 1998; Chinnusamy et al., 2003). To identify the regulatory target genes of TDR, we performed transcriptional analysis of the wild type and the *tdr* mutant anther at the meiosis/young microspore stages using the Affymetrix rice chips (data not shown). From the preliminary data, we identified two genes, Os *CP1* and Os *c6*, for further testing of direct in vivo binding with TDR (Figure 9). Cys proteases (CPs) belong to a family of enzymes found in animals, plants, and microorganisms that play important roles in intracellular protein degradation and are PCD hallmarks (Solomon et al., 1999). Os *CP1* is a rice Cys protease gene, and a loss-of-function mutation in Os *CP1* results in the collapse of microspore after release from tetrads (Lee et al., 2004). The Os *c6* gene encodes a putative protease inhibitor and shows tapetum-specific

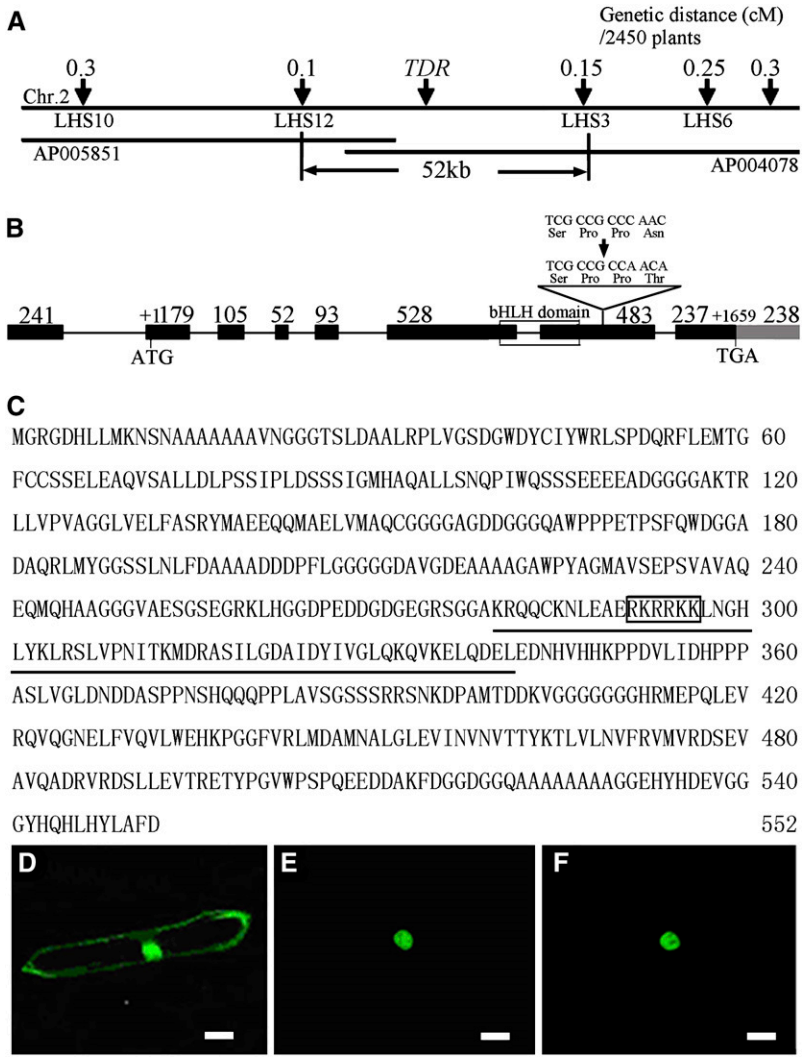

Figure 6. Molecular Identification of *TDR*.

(A) Fine mapping of the *TDR* gene on chromosome 2. Names and positions of the molecular markers are indicated. AP005851 and AP004078 are genomic DNA accession numbers. The *TDR* locus is mapped to a 52-kb region between two molecular markers (LHS12 and LHS3). cM, centimorgan.
(B) A schematic representation of the exon and intron organization of *TDR*. The mutant sequence has one base deletion in the seventh exon. +1 indicates the starting nucleotide of translation, and the stop codon (TAG) is +1659. Black boxes indicate exons, intervening lines indicate introns, the gray box indicates the 3′-untranslated region, and the white box indicates the bHLH domain.
(C) The TDR protein sequence. Putative bHLH domain is underlined. Putative nuclear localization signal is boxed.
(D) A cell that expressed free GFP showing fluorescence in nucleus, cytoplasm, and plasma membrane.
(E) A cell that expressed TDR-GFP showing fluorescence in the nucleus.
(F) Nuclear-localizing AS2 is used as a positive control, and AS2-GFP is exclusively detected in the nucleus. Bars = 20 μm in **(D)** to **(F)**.

expression (Tsuchiya et al., 1992, 1994). Our RT-PCR analysis indicated that Os *CP1* and Os *c6* were expressed in wild-type anthers at the early stages, and their transcripts were greatly reduced as the anther developed into the vacuolated and mature pollen stages. However, reduced Os *CP1* transcript and no expression of Os *c6* were detected in the *tdr* anthers, suggesting that they are possible downstream genes of *TDR* (Figure 9A). Six and four predicted E-box sequences (CANNTG) were also found in the promoter regions of Os *CP1* and Os *c6*, respectively. As a control, three predicted E-box sequences were found in the promoter regions of *Actin1*, which have sequence variation with those of predicted E-box sequences (CANNTG) and were also found in the promoter regions of Os *CP1* and Os *c6* (Figure 9B). Both 514-bp Os *CP1* and 514-bp Os *c6* upstream DNA fragments were specifically enriched when the affinity-purified TDR antibodies were used. However, no enrichment of the 307-bp upstream DNA fragment of *Actin1* was observed using the affinity-purified TDR antibodies (Figure 9C).

To further confirm that TDR has the ability to bind to the promoter regions of Os *CP1* and Os *c6*, EMSA was employed. We

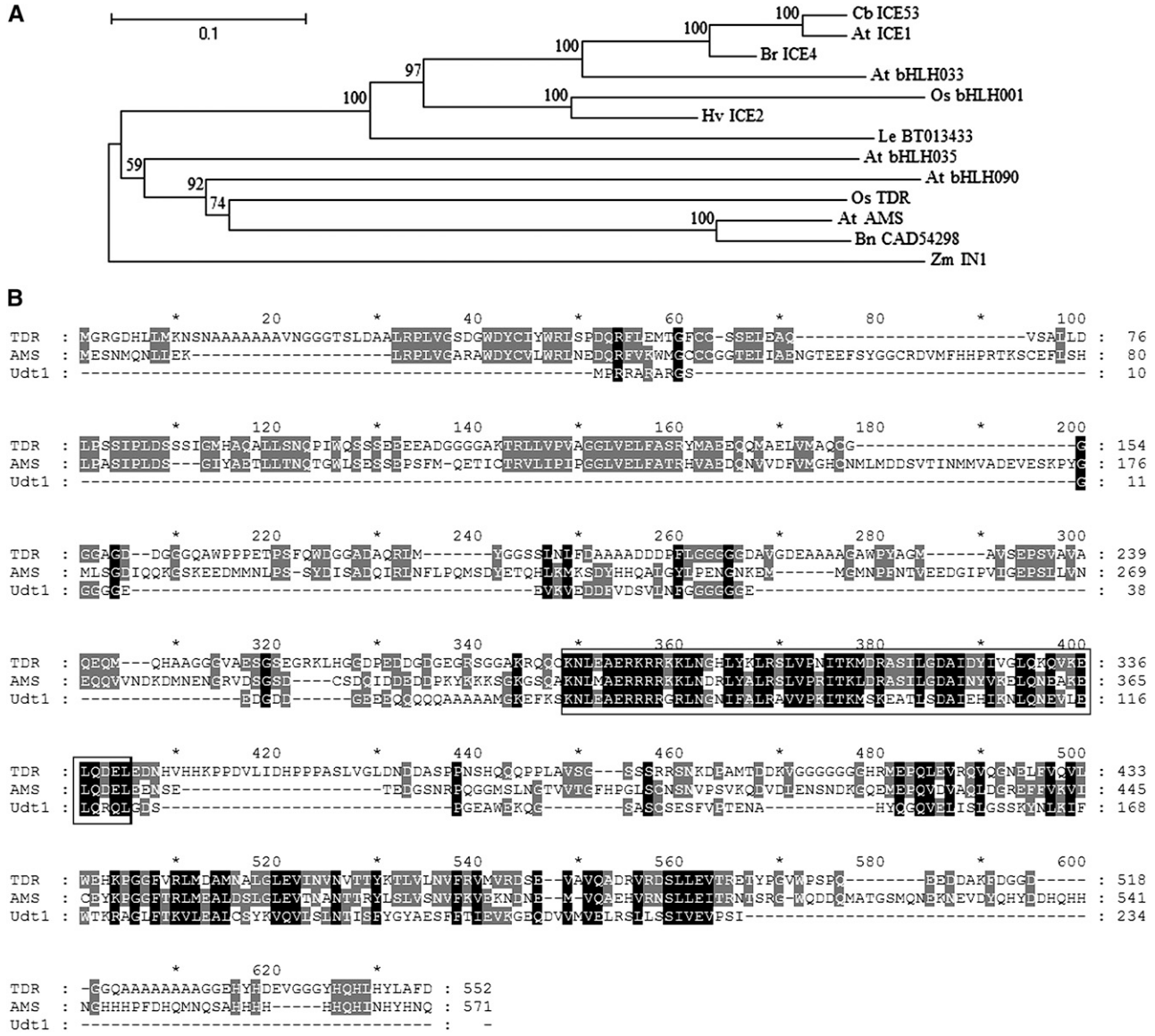

Figure 7. Phylogenetic Analysis of TDR-Related Proteins and Comparison of the Amino Acid Sequences of TDR with AMS and Udt1.

(A) Bootstrap neighbor-joining phylogenetic tree was constructed using MEGA and 1000 replicates. The proteins are named according to their gene names or National Center for Biotechnology Information accession numbers. Zm IN1 is defined as an outgroup. The length of the branches refers to the amino acid variation rates. The alignment on which the tree was constructed is shown in Supplemental Figure 3 online.

(B) The deduced amino acid sequence of TDR is compared with the sequences of AMS and Udt1. bHLH domains are boxed. Black boxes indicate identical residues, and gray boxes indicate similar residues.

observed that TDR could bind the 161-bp DNA fragment (−673 ~ −513) of the Os *CP1* promoter region and the 170-bp DNA fragment (−881 ~ −712) of Os *c6* (data not shown). The DNA binding activities were further tested in the competition experiments by addition of unlabeled DNA fragments as competitors. As shown in Figure 9D, the addition of excess Os *CP1* and Os *c6* competitor DNAs reduced the formation of the complex in a concentration-dependant manner. These results support the hypothesis that TDR directly regulates Os *CP1* and Os *c6* and may regulate tapetum degeneration by upregulating their expression.

DISCUSSION

A Mutation in *TDR* Impairs Rice Anther Development

We report here the characterization of the *TDR* gene in rice. Based on morphological studies, formation of four anther wall cell layers and MMC appeared to be normal. The mutant MMCs entered meiosis and progressed through to the tetrad stage. However, the postmeiotic development of both tapetum and middle layer was disrupted in *tdr* anthers, as indicated by the

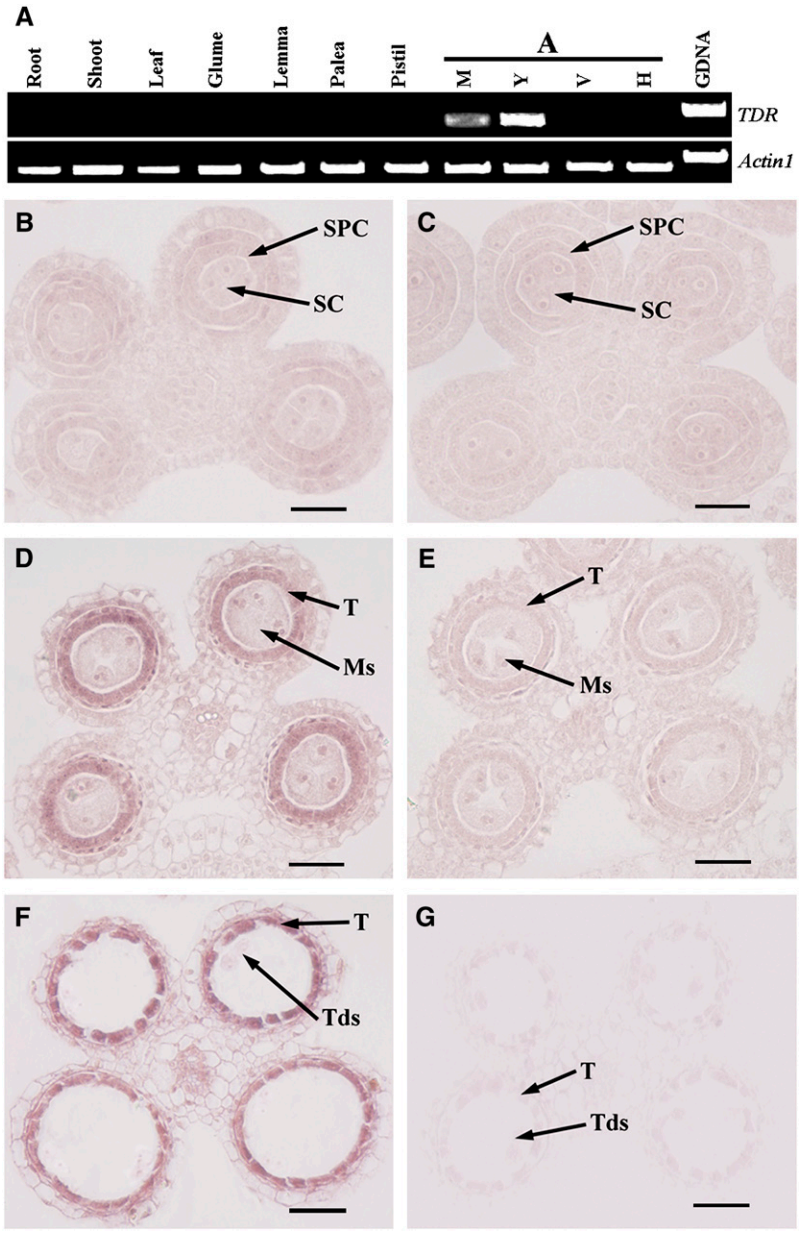

Figure 8. *TDR* Expression Pattern.

(A) Spatial and temporal expression analyses of *TDR* by RT-PCR. M, meiosis; Y, young microspore; V, vacuolated pollen; H, heading stage; GDNA, genomic DNA.
(B) to **(G)** In situ analyses of *TDR*.
(B) A wild-type anther at the early premeiosis stage showing no *TDR* expression.
(C) Successive section to that shown in **(B)**, probed with the *TDR* sense probe.
(D) A meiosis stage wild-type anther showing *TDR* expression in tapetum, middle layer, and endothecium.
(E) A wild-type anther at the meiosis stage with sense probe.
(F) A wild-type anther at the tetrad stage showing stronger *TDR* expression in tapetal cells.
(G) Successive section to that shown in **(F)**, probed with the *TDR* sense probe.
SPC, secondary parietal cell; SC, sporogenous cell; Ms, microsporocytes; T, tapetum; Tds, tetrads. Bars = 25 μm.

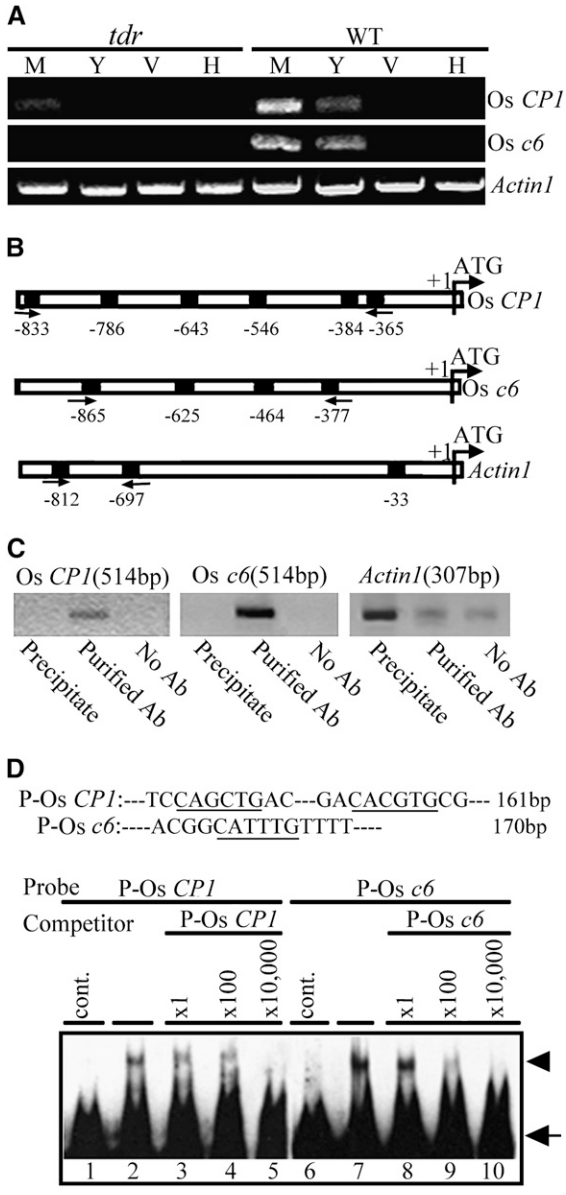

Figure 9. Direct Binding of TDR to the Regulatory Regions of Os *CP1* and Os *c6*.

(A) RT-PCR analyses of Os *CP1* and Os *c6* in wild-type and the *tdr* anthers. M, meiosis; Y, young microspore; V, vacuolated pollen; H, heading stage.

(B) Predicted E-boxes of Os *CP1*, Os *c6*, and *Actin1* within 1-kb upstream regions starting from ATG. The bent arrow denotes the translational start site. The black boxes indicate canonical binding sites for bHLH proteins of the form CANNTG (i.e., E-box). Arrows indicate oligonucleotide primers used in enrichment assays.

(C) Enrichment of the Os *CP1* and Os *c6* regulatory fragments required for the anti-TDR antibody. Enrichment of the Os *CP1* and Os *c6* fragments was only observed when affinity-purified TDR antibody was used, and no *Actin1* fragment was enriched.

(D) TDR was assayed for binding to the regulatory regions of Os *CP1* and Os *c6* in EMSA. The length of DNA probes for Os *CP1* (P-*Os CP1*) and *Os c6* (P-*Os c6*) are 161 and 170 bp, respectively. Dashes represent the omitted nucleotides. The underlined nucleotides indicate E-box. TDR protein was mixed with ^{32}P-labeled Os *CP1* probe (lane 2) and Os *c6* probe (lane 7), and 1-, 100-, and 10,000-fold molar excess of unlabeled Os *CP1* probe (lanes 3 to 5) and Os *c6* probe (lanes 8 to 10) were added as competitor to the EMSA reaction. As a control, translated pET32a control plasmid was added (cont. lanes 1 and 6). An arrow marks free probe. An arrowhead marks supershift band.

appearance of large vacuoles in expanded cells. In addition, microspores collapsed after released from tetrads. Therefore, *TDR* is critical for normal tapetum development and function, which are essential for normal pollen development.

Production of functional pollen grains relies significantly on the timely death and degeneration of the tapetum. Through their degeneration and release of cellular contents, the tapetal cells contribute to the completion of the extracellular sculpting of the pollen grains, providing them with adhesive and signaling molecules of proteinaceous and lipoidal nature that are critical for pollination (Wu et al., 1997; Piffanelli et al., 1998). Using genetic cell ablation, Kawanabe et al. (2006) showed that the PCD signal commences at the tetrad stage, but these authors did not provide cytological evidence of tapetum PCD. In this article, our TUNEL analysis provides direct evidence that the PCD of tapetal cells starts at the tetrad stage. Simultaneously, we also found that the tapetum PCD is retarded in the *tdr* mutant. We propose that the *TDR* gene encodes a key positive regulator of rice tapetum PCD. Combined with TEM observation, we believe that the absence of PCD in the *tdr* mutant tapetum caused a failure to provide critical materials and signals for proper microspore development, resulting in collapse of microspores and male sterility. According to Varnier et al. (2005), anther PCD in *Lilium* is a progressive process that is initiated in the tapetum and then expanded to other anther cell layers. This type of PCD progression can also explain why the lack of PCD in the *tdr* mutant tapetum may further impact the other somatic anther cell layers, such as the middle layer.

How does the *tdr* mutation abolish rice tapetal PCD? In animal systems, the Bcl-2 family proteins are key regulators of both cell survival and cell death (Gross et al., 1999). One member of this family, the mammalian *Bax* gene, has been shown to induce plant PCD that is similar to the PCD associated with the hypersensitive response induced by mosaic virus (Lacomme and Cruz, 1999; Kawai-Yamada et al., 2001). Overexpression of an *Arabidopsis* homolog of human *Bax inhibitor-1* (At *BI-1*) has been shown to block the tapetum PCD, resulting in male sterility (Kawanabe et al., 2006). Although the *tdr* mutation has no effect on the expression of the Os *BI-1* gene (see Supplemental Figure 5 online), our data reveal that the expression of Os *CP1* and Os *c6*, encoding a Cys protease and a proteases inhibitor, respectively, are highly reduced in the *tdr* anthers. Cys proteases and their inhibitors are known to be associated with PCD in various stress responses and during leaf senescence (Minami and Fukuda, 1995; Solomon et al., 1999; Xu and Chye, 1999). Therefore, such Cys proteases likely play crucial roles in tapetum degeneration. Further support for this idea comes from the evidence for a direct regulation of Os *CP1* and Os *c6* by TDR from ChIP and EMSA analyses. Therefore, our data strongly suggest that *TDR*

positively regulates tapetum PCD by controlling tissue-specific effector genes important for PCD.

The *TDR* Gene Is Involved in a Crucial Regulation Network Controlling Postmeiotic Anther Development

The bHLH proteins belong to a superfamily of transcription factors that are important regulatory components in controlling various processes, from cell proliferation to cell lineage establishments. These proteins usually consist of two domains (i.e., a basic domain necessary for DNA binding and a HLH domain for dimerization) (Chinnusamy et al., 2003; Baudry et al., 2004). In plants, bHLH proteins have been reported to regulate a number of biochemical and developmental processes (Murre et al., 1989; Goodrich et al., 1992; Ferre-D'Amare et al., 1994; Kawagoe and Murai, 1996; Abe et al., 1997; Ni et al., 1998; Fairchild et al., 2000; Grandori et al., 2000; Massari and Murre, 2000; Spelt et al., 2000; Heisler et al., 2001; Chinnusamy et al., 2003).

Phylogenetic and BLAST analyses indicate that TDR is most similar to the *Arabidopsis* AMS protein, which is required for male fertility (Sorensen et al., 2003). Additionally, Li et al. (2006) performed phylogenic analysis of 167 rice bHLH genes and 147 *Arabidopsis* bHLH genes, and TDR and AMS also were grouped in the same subfamily. The *AMS* expression starts at a low level premeiotically and increases in postmeiotic anthers. The microspores in the *ams* anther collapse after release from the tetrad, and the tapetum becomes abnormally large and vacuolated at the late stage of anther development, while the middle layer persists (Sorensen et al., 2003). Our results further indicate that the TDR protein is likely localized to the nucleus and has a function similar to that of *AMS*, suggesting the *TDR* is likely the rice ortholog of *AMS*.

Additionally, it is notable that the rice *Udt1* gene encoding a bHLH protein plays a major role in maintaining rice tapetum development at the early meiosis stage. The *udt1* mutation results in the vacuolation and expansion of the tapetal cells from the meiosis stage; the *udt1* meiocytes degenerate at the tetrad stage, and the degeneration of the middle layer is inhibited (Jung et al., 2005). However, the full-length protein sequences of TDR and Udt1 have only 12% identity. In the *udt1* mutant, the transcript of *TDR* is reduced, while the *tdr* mutation has no impact on the expression of *Udt1*. Therefore, *Udt1* is probably upstream of *TDR*. Furthermore, though the expanded tapetum is observed in both *tdr* and *udt1* mutants, the microspore formation occurs only in the *tdr* mutant but not in the *udt1* mutant, which further supports the possibility that *TDR* acts downstream of *Udt1*.

In summary, we show here that *TDR* promotes anther development by positively regulating the tapetum PCD in rice. Also, we further identify two downstream target genes, Os *CP1* and Os *c6*, directly regulated by *TDR*. Our studies have opened a window into the genetic control of postmeiotic tapetum degeneration and development. Recently, it was shown that the *Arabidopsis DYT1* gene encoding a bHLH protein is required for tapetum development and normal levels of *AMS* expression, suggesting that *DYT1* acts upstream of *AMS* (Zhang et al., 2006). Phylogenetic analysis supports the orthology of the *Arabidopsis DYT1* and rice *Udt1* genes (Zhang et al., 2006). Therefore, it is likely that the rice *Udt1-TDR* genes and the *Arabidopsis DYT1-AMS* genes represent an evolutionarily conserved regulatory module critical for normal anther development.

METHODS

Mutant Material and Growth Conditions

The F2 mapping population was generated from a cross between the *tdr* mutant (*japonica*) and LongTeFu B (*indica*). In the F2 population, male sterile plants were selected for gene mapping. All plants were grown in the paddy field of Shanghai Academy of Agriculture Sciences.

Characterization of Mutant Phenotype

Plants or flowers were photographed with a Nikon E995 digital camera and a Motic K400 dissecting microscope. Anther sections were stained by 0.2% 4,6-diamino-2-phenylindole dihydrochloride *n*-hydrate to stain the nuclei. Observation of anther development was performed on standard plastic sections as described by Hong et al. (1995). Spikelets of different developmental stages were collected, based on the length of spikelet, and fixed with 3% (w/v) paraformaldehyde and 0.25% glutaraldehyde in 0.2 N sodium phosphate buffer, pH 7.0, for 20 h at 4°C, rinsed with 0.1 M phosphate buffer, pH 7.0, and dehydrated in an ethanol series. The samples were embedded in Technovit 7100 resin (Hereaus Kulzer), polymerized at 45°C. Transverse sections of 2 μm were cut using an Ultratome III ultramicrotome (LKB) stained with 0.25% toluidine blue O (Chroma Gesellshaft Shaud) and photographed using a Nikon E600 microscope and a Nikon DXM1200 digital camera.

For TEM, spikelets at various stages of development were fixed in 3% (w/v) paraformaldehyde and 0.25% glutaraldehyde in 0.2 N sodium phosphate buffer, pH 7.0, and were postfixed in 2% OsO_4 in PBS, pH 7.2. Following ethanol dehydration, samples were embedded in acrylic resin (London Resin Company). Ultra-thin sections (50 to 70 nm) were double stained with 2% (w/v) uranyl acetate and 2.6% (w/v) lead citrate aqueous solution and examined with a JEM-1230 transmission electron microscope (JEOL) at 80 kV.

Molecular Cloning of *TDR*

For fine-mapping of the *TDR* locus, we developed InDel molecular markers based on the sequence difference between *japonica* variety Nipponbare and *indica* variety 9311 (Jander et al., 2002). The primer sequences of InDel markers were as follows: LHS3 (5′-CACTACTCCCTCTATCGCACG-3′and 5′-ATTATCATTGGATTGACATTTG-3′), LHS6 (5′-AGGTTAGTGCTTCGGAGTGG-3′ and 5′-ACAGACAGAACAGCGGTCAA-3′), LHS10 (5′-CCTTTCAAAGCGCCACAG-3′ and 5′-AGCAGCCGACGTTCCTAA-3′), and LHS12 (5′-CTTGGGGTCTCGCAGCATA-3′ and 5′-GAAGAAGCGGATGAATGGG-3′). PCR amplification and polyacrylamide gel electrophoresis analysis were performed as described previously (Liu et al., 2005).

RT-PCR

Total RNA was isolated using Trizol reagent (Invitrogen) as described by the supplier from rice (*Oryza sativa*) tissues: root shoot, leaf, glume, lemma, palea, and anthers at different stages. The stages of anthers were classified into the following categories according to spikelet length (Feng et al., 2001): meiosis stage anthers within 1- to 3-mm spikelets, young microspore stage anthers within 3- to 5-mm spikelets, vacuolated pollen stage anthers within 5- to 7-mm spikelets, and mature pollen stage anthers within 7- to 8-mm spikelets. After treatment with DNase (Promega), 0.3 μg RNA was used to synthesize the oligo(dT) primed first-strand cDNA

using the ReverTra Ace-α-First Strand cDNA synthesis kit (TOYOBO). Three microliters of the reverse transcription products were subsequently used as template in a PCR reaction. All the primers for RT-PCR are listed in Supplemental Table 1 online.

In Situ Hybridization

Wild-type spikelets of different developmental stages were fixed in 5% acetic acid, 50% ethanol, and 3.7% formaldehyde in water for 16 h at 4°C. They were dehydrated through ethanol series, embedded in Paraplast Plus (Oxford Labware), and sectioned at 8 μm using an YL3-A rotary microtome (Shanghai Instrument Factory). The full-length *TDR* cDNA fragment was digested from the *TDR* cDNA clone vector pCMVFL3 (Rice Genome Resource Center–National Institute of Agrobiological Sciences [RGRC-NIAS]; http://www.rgrc.dna.affrc.go.jp/stock.html) with *Eco*RI or *Bam*HI and was transcribed in vitro under T7 or SP6 promoter with RNA polymerase using the DIG RNA labeling kit (Roche). This mixture was prepared for the DIG-labeled RNA antisense or sense probe. RNA hybridization and immunological detection of the hybridized probes were performed according to the protocol of Kouchi and Hata (1993).

Complementation of the *tdr* Mutant

For functional complementation, an ~6.4-kb genomic DNA fragment containing the entire *TDR* coding region, a 2430-bp upstream sequence, and a 1857-bp downstream sequence was digested from BAC clone AP005851 with *Bam*HI and *Sal*I and subcloned into the binary vector pCAMBIA1301 (CAMBIA) carrying a hygromycin resistance marker to generate p1301TDR construct. We induced the calli using the homogenous *tdr* young panicles, which mainly included palea and lemma, and then the calli were used for transformation with *Agrobacterium tumefaciens* EHA105 carrying the p1301TDR plasmid and the control plasmid p1301.

TDR Nuclear Localization Analysis

The GFP cDNA was amplified from pBSK-GFP vector with the following primers: 5′-aaaaAGATCTATGGGTAAAGGAGAAGAACTTTTCACTG-3′ and 5′-aaaaCACGTGTTAT TTGTATAGTTCATCCATGCCATGTG-3′ (attached restriction site is underlined). The PCR product was cloned into pMD18-T vector (TaKaRa), released by *Bgl*II-*Sma*I digestion, and subcloned into the *Bgl*II-*Pmac*I–digested pCAMBIA1301 vector (CAMBIA) containing 35S promoter to generate p1301-GFP. The *TDR* cDNA was amplified from the cDNA clone vector pCMVFL3 (RGRC-NIAS) with primers 5′-AGTCACGACGTTGTA-3′ and 5′-aaaaAGATCTATCAAACGCGAGGTAATGCAGGTGCT-3′. The amplified fragment was digested with *Nco*I and *Bgl*II and ligated with the same enzyme-digested p1301-GFP to create p1301-TDR-GFP. pAS2-GFP was used as positive control vector (provided by A.-W. Dong, Fudan University, China). The onion epidermis was peeled and bombarded with golden particle–coated plasmids. Cells with GFP fluorescence were observed under a fluorescence confocal microscope (Zeiss LSM 510).

TUNEL

Sections were washed in PBS (160 mM NaCl, 2.7 mM KCl, 8 mM Na_2HPO_4, and 1.5 mM KH_2PO_4) for 5 min and incubated in 20 μg/mL proteinase K in 100 mM Tris-HCl, pH 8.0, and 50 mM Na_2EDTA (100 μL per slide in a humid chamber). The sections were washed in PBS for 5 min and fixed in 4% (w/v) paraformaldehyde in PBS for 10 min, and then the PBS washing was repeated. In situ nick-end labeling of nuclear DNA fragmentation was performed in a humid chamber for 1 h in the dark at 37°C with a TUNEL apoptosis detection kit (DeadEnd Fluorometric TUNEL system; Promega) according to the supplier's instructions. Samples were analyzed under a fluorescence confocal scanner microscope (Zeiss Axioplan).

Comet Assay for DNA Damage

The comet assay kit from Trevigen was used with minor modifications. Anthers of different developmental stages were chopped with a razor in 1.5-mL centrifuge tubes containing 500 μL of ice-cold 1× PBS plus 20 mM EDTA. The resulting mixture was filtered through a 100-μm nylon net filter (Millipore). Thirty microliters of nuclei was mixed with 300 μL of 1% low-melting-point agarose (prewarmed at 37°C) and pipetted onto Trevigen-precoated slides. After incubating in lysis solution at 4°C for 1 h, the slides were dipped in alkaline solution (0.3 N NaOH and 1 mM EDTA) for 30 min and then washed with 1× TBE (Tris-borate/EDTA) three times. The slides were run at 1 V/cm for 10 min in 1× TBE and then dipped in 70% ethanol for 5 min. After air-drying, the slides were stained with a 1:10,000 dilution of SYBR green and then were examined with a Nikon E600 microscope. The percentage of DNA in each comet tail (T DNA%) was evaluated with CometScore software (http://www.autocomet.com). The extent of DNA damage in different samples was derived according to the method described by Wang and Liu (2006).

TDR-Specific Polyclonal Antibody Preparation and Purification

A *TDR*-specific fragment was amplified from cDNA clone vector pCMVFL3 (RGRC-NIAS) using the primer pairs N12F (5′-aaaGAATTCAACAGCCACCAACAGCAGC-3′) and N12R (5′-aaaAAGCTTTCATCAATCAAACGCGAGGTAATGC-3′). The PCR product was cloned into the *Eco*RI and *Hin*dIII sites of pET-32a vector (Novagen) to produce p32-TDR. The fusion protein expression and purification were performed according to the manual of pET-32a from Novagen, and antibody preparation was performed as described by Huang et al. (2003).

ChIP and Enrichment Test for in Vivo Binding of TDR

The procedure for ChIP of TDR-DNA complexes in rice wild-type anther was modified from Bowler et al. (2004). Briefly, rice anthers at the meiosis stage were treated with formaldehyde, and the chromatin solution was sonicated on an Ultrasonic Crasher Noise Isolating Chamber (SCIENTZ). The soluble chromatin fragments were obtained from isolated nuclei. Preadsorption with sheared salmon sperm DNA/protein A agarose mix (Sigma-Aldrich) was performed to remove nonspecific binding DNA. Immunoprecipitation with TDR-specific immune antiserum and preadsorption with protein A-Sepharose beads and without any serum were performed as in the reference above.

Oligonucleotide primers specific for the upstream of Os *CP1* (5′-CCTAAAGAAGCAGTTGCCAT-3′ and 5′-GATTGGGGATTGAGGTGTTA-3′), Os *c6* (5′-CAACGAACGGCATTTGTTTT-3′ and 5′-GACTTTTTAGCACATGTTTA-3′), and *Actin1* (5′-GTTCCTAAAGCCCAAAGTGC-3′ and 5′-TGTATATAGTGGCGATGGGG-3′) were added to PCR reactions in which the templates were ChIP populations from immune or control immunoprecipitations. Typically, 34 cycles of PCR were performed, and the products were analyzed by agarose gel electrophoresis.

EMSA

The DNA fragments containing the E-box of the Os *CP1* and Os *c6* regulatory region were generated using PCR amplification with the following specific primers: P-*Os CP1* (5′-TTCCCCTTCCACCAAAAACG-3′ and 5′-AAATCTAGGCGAGACTCCAC-3′) and P-*Os c6* (5′-CAACGAACGGCATTTGTTTT-3′ and 5′-GCAGGAACTAATTAAATAAGTTTGT-3′). The two DNA fragments were cloned into pMD18-T vector

(TaKaRa) for sequence confirmation. The specific primers (25 pmol/μL) were incubated with polynucleotide kinase (Promega), 10× polynucleotide kinase buffer, and ^{32}P-dATP at 37°C for 30 min and labeled with ^{32}P. The two inserts were labeled with ^{32}P through PCR with ^{32}P-labeled specific primers and purified on an 8% PAGE gel.

Full-length *TDR* was amplified from cDNA clone vector pCMVFL3 (RGRC-NIAS) using the primer pairs 32a-F (5′-GAATTCATGGGAAGAGGAGACCACC-3′) and 32a-R (5′-GTCGACTGGTAAAATCAATCATCATC-3′). The PCR product was cloned into the pMD18-T vector (TaKaRa) and released by *Eco*RI and *Sal*I digestion. This fragment was then ligated with the same enzyme-digested pET32a (Novagen). The fusion protein was expressed in *Escherichia coli* as described by Huang et al. (2003).

The DNA binding reactions were performed according to Wang et al. (2002) with the following modifications. Reaction components were incubated in 1× binding buffer [10 mM Tris-HCl, pH 7.5, 50 mM NaCl, 1 mM EDTA, 5% glycerol, 0.05 μg μL^{-1} poly(dI-dC), and 0.1 μg μL^{-1} BSA] at room temperature for 20 min. The entire reaction mix was analyzed on a 3.5% PAGE gel. After drying the gel, ^{32}P-labeled DNA fragments were detected using an autoradiograph.

Computational and Database Analysis

A phylogenetic tree was constructed with the aligned plant bHLH protein sequences using MEGA software (version 3.0) (http://www.megasoftware.net/index.html) (Kumar et al., 2004) based on the neighbor-joining method with the following parameters: p-distance model, pairwise deletion, and bootstrap (1000 replicates; random seed). The multiple alignments were performed using ClustalW (http://www.ebi.ac.uk/clustalw/).

Accession Numbers

Sequence data from this article for the cDNA and genomic DNA of *TDR* can be found in the GenBank/EMBL data libraries under accession numbers XM_463907 and AP004078, respectively.

Supplemental Data

The following materials are available in the online version of this article.

Supplemental Table 1. List of the Primers Used for RT-PCR Analyses.

Supplemental Figure 1. Results of DAPI Staining to Detect Nuclei.

Supplemental Figure 2. Complementation of the *tdr* Mutant by *TDR* Genomic DNA.

Supplemental Figure 3. Sequence Alignment of TDR and 12 TDR-Related bHLH Proteins.

Supplemental Figure 4. Expression Analysis of *Udt1*.

Supplemental Figure 5. Expression Analysis of Os *Bl-1*.

ACKNOWLEDGMENTS

We thank B. Han (Rice Genome Resource Center) and A.-W. Dong for providing the BAC clone, cDNA clone, and pAS2-GFP plasmid. We thank Z.-J. Luo and M.-J. Chen for mutant screening and generation of F2 populations for the mapping, C.-M. Zhang for rice transformation, Y.-J. Lu for plastic sections, X.-S. Gao and K.-Y. Chen for confocal microscope imaging, and Q. Song for TEM observation. Z.-C. Liu is gratefully acknowledged for her valuable suggestions regarding ChIP and comet assay experiments and helpful comments on the manuscript. We are also grateful to H. Yu for editing this manuscript. This work was supported by funds from the National Key Basic Research Developments Program of the Ministry of Science and Technology, People's Republic of China (2006CB101700 and 2005CB120802), the National "863" High-Tech Project (2005AA2710330), the Program for New Century Excellent Talents in University (NCET-04-0403), the Shuguang Scholarship (04SG15), and the Shanghai Institutes of Biological Sciences (Reproductive Development Project).

Received May 13, 2006; revised October 11, 2006; accepted November 2, 2006; published November 30, 2006.

REFERENCES

Abe, H., Yamaguchi-Shinozaki, K., Urao, T., Iwasaki, T., Hosokawa, D., and Shinozaki, K. (1997). Role of *Arabidopsis* MYC and MYB homologs in drought- and abscisic acid-regulated gene expression. Plant Cell **9,** 1859–1868.

Albrecht, C., Russinova, E., Hecht, V., Baaijens, E., and de Vries, S. (2005). The *Arabidopsis thaliana* SOMATIC EMBRYOGENESIS RECEPTOR-LIKE KINASES1 and 2 control male sporogenesis. Plant Cell **17,** 3337–3349.

Baudry, A., Heim, M.A., Dubreucq, B., Caboche, M., Weisshaar, B., and Lepiniec, L. (2004). TT2, TT8, and TTG1 synergistically specify the expression of BANYULS and proanthocyanidin biosynthesis in *Arabidopsis thaliana.* Plant J. **39,** 366–380.

Bouchard, C., Staller, P., and Eilers, M. (1998). Control of cell proliferation by Myc. Trends Cell Biol. **8,** 202–206.

Bowler, C., Benvenuto, G., Laflamme, P., Molino, D., Probst, A.V., Tariq, M., and Paszkowski, J. (2004). Chromatin techniques for plant cells. Plant J. **39,** 776–789.

Canales, C., Bhatt, A.M., Scott, R., and Dickinson, H. (2002). EXS, a putative LRR receptor kinase, regulates male germline cell number and tapetal identity and promotes seed development in *Arabidopsis.* Curr. Biol. **12,** 1718–1727.

Chinnusamy, V., Ohta, M., Kanrar, S., Lee, B., Hong, X., Agarwal, M., and Zhu, J.K. (2003). ICE1: A regulator of cold-induced transcriptome and freezing tolerance in *Arabidopsis.* Genes Dev. **17,** 1043–1054.

Colcombet, J., Boisson-Dernier, A., Ros-Palau, R., Vera, C.E., and Schroeder, J.I. (2005). *Arabidopsis* SOMATIC EMBRYOGENESIS RECEPTOR KINASES1 and 2 are essential for tapetum development and microspore maturation. Plant Cell **17,** 3350–3361.

Endo, M., Tsuchiya, T., Saito, H., Matsubara, H., Hakozaki, H., Masuko, H., Kamada, M., Higashitani, A., Takahashi, H., Fukuda, H., Demura, T., and Watanabe, M. (2004). Identification and molecular characterization of novel anther-specific genes in *Oryza sativa* L. by using cDNA microarray. Genes Genet. Syst. **79,** 213–226.

Fairchild, C.D., Schumaker, M.A., and Quail, P.H. (2000). *HFR1* encodes an atypical bHLH protein that acts in phytochrome A signal transduction. Genes Dev. **14,** 2377–2391.

Feng, J.H., Lu, Y.G., Liu, X.D., and Xu, X.B. (2001). Pollen development and its stages in rice (*Oryza sativa* L.). Chinese J. Rice Sci. **15,** 21–28.

Ferre-D'Amare, A.R., Pognonec, P., Roeder, R.G., and Burley, S.K. (1994). Structure and function of the b/HLH/Z domain of USF. EMBO J. **13,** 180–189.

Goldberg, R.B., Beals, T.P., and Sanders, P.M. (1993). Anther development: Basic principles and practical applications. Plant Cell **5,** 1217–1229.

Goodrich, J., Carpenter, R., and Coen, E.S. (1992). A common gene regulates pigmentation pattern in diverse plant species. Cell **68,** 955–964.

Grandori, C., Cowley, S.M., James, L.P., and Eisenman, R.N. (2000). The Myc/Max/Mad network and the transcriptional control of cell behavior. Annu. Rev. Cell Dev. Biol. **16,** 653–699.

Gross, A., McDonnell, J.M., and Korsmeyer, S.J. (1999). BCL-2 family members and the mitochondria in apoptosis. Genes Dev. **13,** 1899–1911.

Heisler, M.G.B., Atkinson, A., Bylstra, Y.H., Walsh, R., and Smyth, D.R. (2001). *SPATULA*, a gene that controls development of carpel margin tissues in *Arabidopsis*, encodes a bHLH protein. Development **128,** 1089–1098.

Higginson, T., Li, S.F., and Parish, R.W. (2003). *AtMYB103* regulates tapetum and trichome development in *Arabidopsis thaliana.* Plant J. **35,** 177–192.

Hong, S.K., Aoki, T., Kitano, H., Satoh, H., and Nagato, Y. (1995). Phenotypic diversity of 188 rice embryo mutants. Dev. Genet. **16,** 298–310.

Huang, Y.H., Liang, W.Q., Pan, A.H., Zhou, Z.A., Huang, C., Chen, J.X., and Zhang, D.B. (2003). Production of FaeG, the major subunit of K88 fimbriae, in transgenic tobacco plants and its immunogenicity in mice. Infect. Immun. **71,** 5436–5439.

Jander, G., Norris, S.R., Rounsley, S.D., Bush, D.F., Levin, I.M., and Last, R.L. (2002). *Arabidopsis* map-based cloning in the post-genome era. Plant Physiol. **129,** 440–450.

Jung, K.H., Han, M.J., Lee, Y.S., Kim, Y.W., Hwang, I., Kim, M.J., Kim, Y.K., Nahm, B.H., and An, G. (2005). Rice Undeveloped Tapetum1 is a major regulator of early tapetum development. Plant Cell **17,** 2705–2722.

Kapoor, S., Kobayashi, A., and Takatsuji, H. (2002). Silencing of the tapetum-specific zinc finger gene *TAZ1* causes premature degeneration of tapetum and pollen abortion in *Petunia.* Plant Cell **14,** 2353–2367.

Kawagoe, Y., and Murai, N. (1996). A novel basic region/helix-loophelix protein binds to a G-box motif CACGTG of the bean seed storage protein b-phaseolin gene. Plant Sci. **116,** 47–57.

Kawai-Yamada, M., Jin, L., Yoshinaga, K., Hirata, A., and Uchimiya, H. (2001). Mammalian Bax-induced plant cell death can be down-regulated overexpression of *Arabidopsis Bax Inhibitor* (*AtBI-1*). Proc. Natl. Acad. Sci. USA **98,** 12295–12300.

Kawanabe, T., Ariizumi, T., Kawai-Yamada, M., Uchimiya, H., and Toriyama, K. (2006). Abolition of tapetum suicide program ruins microsporogenesis. Plant Cell Physiol. **47,** 784–787.

Kouchi, H., and Hata, S. (1993). Isolation and characterization of novel nodulin cDNAs representing genes expressed at early stages of soybean nodule development. Mol. Gen. Genet. **238,** 106–119.

Kumar, S., Tamura, K., and Nei, M. (2004). MEGA3: Integrated software for molecular evolutionary genetics analysis and sequence alignment. Brief. Bioinform. **5,** 150–163.

Lacomme, C., and Cruz, S.S. (1999). Bax-induced cell death in tobacco is similar to the hypersensitive response. Proc. Natl. Acad. Sci. USA **96,** 7956–7961.

Lee, S., Jung, K.H., An, G., and Chung, Y.Y. (2004). Isolation and characterization of a rice cysteine protease gene, *Os CP1*, using T-DNA gene-trap system. Plant Mol. Biol. **54,** 755–765.

Li, X.X., et al. (2006). Genome-wide analysis of basic/helix-loop-helix transcription factor family in rice and *Arabidopsis.* Plant Physiol. **141,** 1167–1184.

Liu, H.S., et al. (2005). Genetic analysis and mapping of rice (*Oryza sativa* L.) male-sterile (OsMS-L) mutant. Chin. Sci. Bull. **50,** 38–41.

Ma, H. (2005). Molecular genetic analyses of microsporogenesis and microgametogenesis in flowering plants. Annu. Rev. Plant Biol. **56,** 393–434.

Massari, M.E., and Murre, C. (2000). Helix-loop-helix proteins: Regulators of transcription in eukaryotic organisms. Mol. Cell. Biol. **20,** 429–440.

McCormick, S. (1993). Male gametophyte development. Plant Cell **5,** 1265–1275.

Minami, A., and Fukuda, H. (1995). Transient and specific expression of a cysteine endopeptidase associated with autolysis during differentiation of *Zinnia* mesophyll cells into tracheary elements. Plant Cell Physiol. **36,** 1599–1606.

Murre, C., McCaw, P.S., and Baltimore, D. (1989). A new DNA binding and dimerization motif in immunoglobulin enhancer binding, daughterless, MyoD and myc proteins. Cell **56,** 777–783.

Ni, M., Tepperman, J.M., and Quail, P.H. (1998). PIF3, a phytochromeinteracting factor necessary for normal photoinduced signal transduction, is a novel basic helix-loop-helix protein. Cell **95,** 657–667.

Nonomura, K.I., Miyoshi, K., Eiguchi, M., Suzuki, T., Miyao, A., Hirochika, H., and Kurata, N. (2003). The *MSP1* gene is necessary to restrict the number of cells entering into male and female sporogenesis and to initiate anther wall formation in rice. Plant Cell **15,** 1728–1739.

Owen, H.A., and Makaroff, C.A. (1995). Ultrastructure of microsporogenesis and microgametogenesis in *Arabidopsis thaliana* (L.) Heynh. ecotype Wassilewskija (*Brassicaceae*). Protoplasma **185,** 7–21.

Pacini, E., Franchi, G.G., and Hesse, M. (1985). The tapetum: Its form, function, and possible phylogeny in Embryophyta. Plant Syst. Evol. **149,** 155–185.

Papini, A., Mosti, S., and Brighigna, L. (1999). Programmed-cell death events during tapetum development of angiosperms. Protoplasma **207,** 213–221.

Piffanelli, P., Rose, J.H., and Murphy, D.J. (1998). Biogenesis and function of the lipidic structures of pollen grains. Sex. Plant Reprod. **11,** 65–80.

Raghavan, V. (1997). Anther developmental biology. In Molecular Embryology of Flowering Plants, V. Raghavan, ed (Cambridge, UK: Cambridge University Press), pp. 17–60.

Scott, R., Hodge, R., Paul, W., and Draper, J. (1991). The molecular biology of anther differentiation. Plant Sci. **80,** 167–191.

Shivanna, K.R., Cresti, M., and Ciampolini, F. (1997). Pollen development and pollen-pistil interaction. In Pollen Biotechnology for Crop Production and Improvement, K.R. Shivanna and V.K. Sawhney, ed (Cambridge, UK: Cambridge University Press), pp. 15–39.

Solomon, M., Belenghi, B., Delledonne, M., Menachem, E., and Levine, A. (1999). The involvement of cysteine proteases and protease inhibitor genes in the regulation of programmed cell death in plants. Plant Cell **11,** 431–443.

Sorensen, A.M., Kröber, S., Unte, U.S., Huijser, P., Dekker, K., and Saedler, H. (2003). The *Arabidopsis ABORTED MICROSPORES* (*AMS*) gene encodes a MYC class transcription factor. Plant J. **33,** 413–423.

Spelt, C., Quattrocchio, F., Mol, J.N.M., and Koes, R. (2000). *Anthocyanin1* of petunia encodes a basic helix-loop-helix protein that directly activates transcription of structural anthocyanin genes. Plant Cell **12,** 1619–1631.

Tsuchiya, T., Toriyama, K., Ejiri, S., and Hinata, K. (1994). Molecular characterization of rice genes specially expressed in the anther tapetum. Plant Mol. Biol. **26,** 1737–1746.

Tsuchiya, T., Toriyama, K., Nasrallah, M.E., and Ejiri, S. (1992). Isolation of genes abundantly expressed in rice anthers at the microspore stage. Plant Mol. Biol. **20,** 1189–1193.

Varnier, A.L., Mazeyrat-Gourbeyre, F., Sangwan, R.S., and Clement, C. (2005). Programmed cell death progressively models the development of anther sporophytic tissues from the tapetum and is triggered in pollen grains during maturation. J. Struct. Biol. **152,** 118–128.

Wang, C., and Liu, Z. (2006). Arabidopsis ribonucleotide reductases are critical for cell cycle progression, DNA damage repair, and plant development. Plant Cell **18,** 350–365.

Wang, H., Tang, W., Zhu, C., and Perry, S.E. (2002). A chromatin immunoprecipitation (ChIP) approach to isolate genes regulated by AGL15, a MADS domain protein that preferentially accumulates in embryos. Plant J. **32,** 831–843.

Wilson, Z.A., Morroll, S.M., Dawson, J., Swarup, R., and Tighe, P.J. (2001). The *Arabidopsis MALE STERILITY1* (*MS1*) gene is a transcriptional regulator of male gametogenesis, with homology to the PHD finger family of transcription factors. Plant J. **28,** 27–39.

Wu, H.M., and Cheung, A.Y. (2000). Programmed cell death in plant reproduction. Plant Mol. Biol. **44,** 267–281.

Wu, S.S., Platt, K.A., Ratnayake, C., Wang, T.W., Ting, J.T., and Huang, A.H. (1997). Isolation and characterization of neutral-lipid-containing organelles and globuli-filled plastids from *Brassica napus* tapetum. Proc. Natl. Acad. Sci. USA **94,** 12711–12716.

Xu, F.X., and Chye, M.L. (1999). Expression of cysteine proteinase during developmental events associated with programmed cell death in *brinjal*. Plant J. **17,** 321–327.

Yang, S.L., Jiang, L., Puah, C.S., Xie, L.F., Zhang, X.Q., Chen, L.Q., Yang, W.C., and Ye, D. (2005). Overexpression of *TAPETUM DETERMINANT1* alters the cell fates in the *Arabidopsis* carpel and tapetum via genetic interaction with excess microsporocytes1/extra sporogenous cells. Plant Physiol. **139,** 186–191.

Yang, S.L., Xie, L.F., Mao, H.Z., Pauh, C.S., Yang, W.C., Jiang, L., Sundaresan, V., and Ye, D. (2003). *TAPETUM DETERMINANT1* is required for cell specialization in the *Arabidopsis* anther. Plant Cell **15,** 2792–2804.

Zhang, W., Sun, Y., Timofejeva, L., Chen, C., Grossniklaus, U., and Ma, H. (2006). Control of *Arabidopsis* tapetum development by *DYSFUNCTIONAL TAPETUM 1* (*DYT1*) encoding a putative bHLH transcription factor. Development **133,** 3085–3095.

Zhao, D.Z., Wang, G.F., Speal, B., and Ma, H. (2002). The *EXCESS MICROSPOROCYTES1* gene encodes a putative leucine-rich repeat receptor protein kinase that controls somatic and reproductive cell fates in the *Arabidopsis* anther. Genes Dev. **16,** 2021–2031.